QTR-FRET: Efficient Background Reduction Technology in Time-Resolved Förster Resonance Energy Transfer Assays

Markku Syrjänpää,[1,#] Emmiliisa Vuorinen,[2] Sakari Kulmala,[3] Qi Wang,[1] Harri Härmä,[2] and Kari Kopra[2,*]

[1] Institute of Biomedicine, Department of Cell Biology and Anatomy, Laboratory of Biophysics, University of Turku, Tykistökatu 6A, FI-20520 Turku, Finland.

[2] Materials Chemistry and Chemical Analysis, Department of Chemistry, University of Turku, Vatselankatu 2, FI-20500 Turku, Finland.

[3] Laboratory of Analytical Chemistry, Department of Chemistry, Aalto University, P.O. Box 16100, FI-00076 Aalto, Finland.

[#] Current address: Abacus Diagnostica Ltd., Tykistökatu 4D, FI-20520 Turku, Finland.

Abstract

A novel homogeneous assay system QTR-FRET (Quencher modulated Time-Resolved Förster Resonance Energy Transfer) combining quenching resonance energy transfer (QRET) and time-resolved Förster resonance energy transfer (TR-FRET) was developed to reduce background signal in the conventional energy transfer applications. The TR-FRET functionality is often limited by the lanthanide donor background signal leading to the use of low donor concentration. QTR-FRET reduces this background by introducing soluble quencher molecule, and in this work the concept functionality was proven and compared to previously introduced QRET and TR-FRET technologies. Comparison was performed with three different Eu^{3+}-chelates exhibiting different luminescent lifetime and stability. The side-by-side comparison of the three signaling systems and Eu^{3+}-chelates was demonstrated in a model assay with Eu^{3+}-chelate conjugated biotin and streptavidin (SA) or Cy5-SA conjugate. Comparison of the methodologies showed increased signal-to-background ratios when comparing QTR-FRET to TR-FRET, especially at high Eu^{3+}-biotin concentrations. Quenching the non-bound Eu^{3+}-biotin improved the assay performance, which

suggests that an improved assay performance can be attained with the QTR-FRET method. QTR-FRET is expected to be especially useful for Eu^{3+}-labeled ligands with low affinity or assays requiring high Eu^{3+}-ligand concentration. The QTR-FRET indicated potential for multi-analyte approaches separately utilizing the direct QRET-type Eu^{3+}-chelate signal and energy transfer signal readout in a single-well. This potential was hypothesized with Avi-KRAS nucleotide exchange assay as a second biologically relevant model system.

1. Introduction

Homogeneous assays exploiting Förster resonance energy transfer (FRET) are popular in the fields of cell biology, diagnostic assays, and drug discovery [1-3]. FRET is described as nonradiative energy transfer between two light-sensitive molecules, donor and acceptor. This process is extremely sensitive to the distance between the used fluorophores, and also relies on spectral overlap between donor emission and acceptor excitation spectra [1-3]. Using long emission lifetime donors, e.g. lanthanide chelates, the energy transfer technique can be significantly improved and the enhanced sensitivity has been utilized for various applications [4-9]. Many molecules in biological fluids are intrinsically fluorescent, which limits the use of conventional fluorophores in detection. Long emission lifetime of the donor enables time-gated FRET (TR-FRET) measurements within a time scale sufficiently long to eliminate direct acceptor and matrix fluorescence. Compared to conventional fluorophores, lanthanide chelates possess a large shift between emission and excitation maximum. Chelates also enable the use of increased distance between donor and acceptor fluorophores without losing its energy transfer efficiency as quickly as in conventional FRET process with organic fluorophores [4-9].

Lanthanides, e.g. Eu^{3+} and Tb^{3+}, are very weakly luminescent as ions, but can form highly luminescent complexes with protective and light harvesting ligands. Non-luminescent lanthanide chelates have been extensively used in dissociative fluorescence enhancement (DELFIA) with femtomolar detection limit [10,11]. Intrinsically signaling lanthanide chelates can circumvent the need for enhancement step and enable homogeneous assays and energy transfer applications [4-6]. However, the synthesis of these chelates is relatively complex increasing the price of these labels. Directly luminescent Eu^{3+}-chelates are highly suitable and often used as a donor in various energy transfer applications [4-9,12-16]. Efficiency of varying energy transfer technologies is limited by non-specific interactions between donor and acceptor fluorophores or their conjugates and direct donor emission counted in the acceptor emission window. These problems can be partly solved by careful fluorophore-pair and measurement optics optimization, but especially the need for high

lanthanide donor concentrations might reduce the assay functionality. Typically, low concentrations of chelate conjugated ligands used in biochemical assays are desirable. However, impure chelate-conjugated ligand resulting from challenging purification, or low affinity ligand needed at high concentrations, force the use of high concentration of labeled ligand in receptor-ligand binding studies. Keeping these problems in mind, non-conventional FRET and TR-FRET assays has been developed to enable the use of partially impure ligands and enable the use of spectrally non-overlapping fluorophores [17-20].

We have previously reported new synthesis route to enhance the temperature and pH stability of a conventional 7-dentate Eu^{3+}-chelate [21]. The new 9- and 11-dentate Eu^{3+}-chelates have longer emission lifetime and improved sensitivity compared to previous 7-dentate chelate, when tested in a heterogeneous CRP fluoroimmunoassay [21]. We have also reported a single-label quenching resonance energy transfer (QRET) concept utilizing an intrinsically luminescent Eu^{3+}-chelate labeled small molecule and soluble quencher [15,22]. The QRET technique combines the sensitivity of the time-resolved luminescence (TRF) detection to single-label concept, simplifying the conventional TR-FRET approach where both used fluorophores are individually conjugated to ligand and receptor. In the QRET, free labeled molecule is quenched by soluble quencher, while the lanthanide chelate TRF-signal is partially protected from quenching after binding to its receptor. Partial protection is due to the difference between quenched and protected label emission lifetimes [23]. Thus, time-gated measurement is necessary for specific signal counting in competitive or non-competitive homogeneous QRET assay format [15,22,23].

In this article we propose an improvement to the conventional TR-FRET technique by combining the TR-FRET and QRET methods. In the novel signaling technique named as QTR-FRET (Quencher modulated Time-Resolved Förster Resonance Energy Transfer), soluble quencher is introduced to the traditional TR-FRET reaction to reduce the background signal resulting from nonspecific energy transfer between donor and acceptor or lanthanide donor emission leaking to measurement window. This approach is expected to be especially useful with low affinity ligands requiring high concentration of Eu^{3+}-ligand. The QTR-FRET approach was demonstrated by comparing three Eu^{3+}-chelates, 7-, 9- and 11-dentate, side-by-side in the homogeneous biotin-streptavidin (SA) assay. Same assays were also performed with TR-FRET and QRET approaches to highlight the improved functionality of the QTR-FRET method. The SA-biotin model assay was chosen to minimize the affinity related issues and to show the quenching effect in the conventional TR-FRET assay. QTR-FRET and QRET techniques showed similar preference to more stable 9-dentate chelate, as the TR-FRET preferred the 7-dentate Eu^{3+}-chelate. Using Avi-KRAS as a second

target we confirmed the QTR-FRET improved functionality over TR-FRET and methods preference for 9-dentate Eu^{3+}-chelate. Results also indicate potential QTR-FRET applicability for multi-analyte approaches.

2. Materials and methods

2.1 Materials and Chemicals

Black OptiPlate 384-well plates, clear SpectraPlate 96-well plates, $EuCl_3$ standard, and DELFIA enhancement solution (DES) were purchased from PerkinElmer Life and Analytical Sciences, Wallac (Turku, Finland). Black Corning round bottom low volume 384-well plates used in emission and excitation spectra characterizations and Avi-KRAS assays were from Corning (Kennebunk, ME). The soluble quencher molecule, MT2, was obtained from QRET Technologies (Turku, Finland) and used according to manufacturer's instruction. Cy5 *N*-hydroxysuccinimide ester (NHS) and NAP-5 gel filtration columns were from GE healthcare (Uppsala, Sweden). Alexa Fluor 680 NHS was purchased from Life Technologies, Thermo Fisher Scientific (Darmstadt, Germany). SA was purchased from BioSpa (Milan, Italy). Eu^{3+}-chelates were synthetized in-house and conjugated through isothiocyanate (ITC) chemistry [21]. The 2′/3′-AHC-GTP (2′-/3′-O-(6-aminohexylcarbamoyl)guanosine-5′-O-triphosphate) was purchased from BIOLOG Life Science Institute (Bremen, Germany). Avi-tagged KRAS (Avi-KRAS, aa 1-188) was co-expressed as a TEV-cleavable MBP fusion with the biotinligase BirA in *Escherichia coli*, and it was a kind gift from Jonas Kapp (University of Zurich, Switzerland). His-SOS^cat (aa 564-1049) protein was of human origin and produced in *Escherichia coli*, and it was a kind gift from Dr. William Gillette (Leidos Biomedical Research, Inc., Frederick National Laboratory for Cancer Research, Frederick, USA). All other reagents, including analytical-grade solvents, *N*-biotinyl-3-aminopropylammonium trifluoroacetate, biotin, malachite green (MG), γ-globulins, and albumin from bovine serum (BSA) were from Sigma-Aldrich (St. Louis, MO).

2.2 Instrumentation

The Eu(III)-biotin purification was carried out using reversed-phase adsorption chromatography, Dionex ultimate 3000 LC system from Thermo Fischer Scientific, Dionex (Sunnyvale, CA), and Ascentis RP-amide C18 column from Sigma-Aldrich, Supelco Analytical (St. Louis, MO). Luminescence signals were measured with a Victor 1420 multilabel counter from PerkinElmer Life and Analytical Sciences, Wallac or Spark 20M from Tecan Life Sciences (Männedorf, Switzerland). All assays were performed in 384-well plate format. In the QRET assays, the Eu^{3+} emission signals were measured at 615 nm, using 340 nm excitation wavelength and 400 μs delay

and integration times. In the TR-FRET with Cy5, the time-resolved emission signals were measured at 665 nm using 75 µs delay and integration times. TR-FRET with Alexa680 was monitored at 740 nm using 75 µs delay and 400 µs integration times. In all TR-FRET and QTR-FRET assays the excitation wavelength 340 nm was used. Emission and excitation spectra for Cy5-SA, Eu^{3+}-chelates (bio7, bio9 and bio11), and absorption spectra for quenchers (MG and MT2) were monitored using Tecan Spark 20M.

2.3 Eu^{3+}-biotin and Eu^{3+}-GTP preparation

Synthesis of 7-, 9-, and 11-dentate Eu^{3+}-chelates carrying an ITC-group and preparation of their biotin-complexes bio7, bio9, and bio11 were performed as described before [21]. The concentration of the purified bio7, bio9, and bio11 was determined from Eu^{3+}-ion concentration utilizing DELFIA technique and comparing the signal to the 1 nM $EuCl_3$ standard in DES. Bio7, bio9, and bio11 were first diluted to 5 M HCl to dissociate the Eu^{3+}-ion, and further diluted to DES to re-chelate the free Eu^{3+}-ion and to compare it to the standard free Eu^{3+}-ion solution. Preparation of 7- and 9-dentate Eu^{3+}-chelate conjugates (GTP-Eu7 and GTP-Eu9) with GTP were performed as described before, and concentrations were monitored as with Eu^{3+}-biotin conjugates [24].

2.4 Cy5-SA preparation

Cy5 and Alexa680 *N*-hydroxysuccinimide ester labels were conjugated to streptavidin to prepare Cy5-SA. Streptavidin (0.5 mg) was labeled with two-fold molar excess of Cy5 *N*-hydroxysuccinimide ester in 50 µL. Overnight reaction was performed in 50 mM carbonate buffer pH 8.3 at room temperature in dark. Cy5-SA conjugate was purified using NAP-5 column according to the instructions of the manufacturer. The labeling degree of Cy5-SA and Alexa680-SA were determined based on the monitored absorbance at 280 nm and 680 nm or 705 nm for Cy5-SA and Alexa680-SA, respectively.

2.5 Spectral characterization

TRF excitation spectra (230–400 nm) for Eu^{3+}-chelate biotin conjugates were monitored with 20 nm slit, 612 nm emission using 10 nm slit, 50 µs delay and 400 µs integration times. TRF emission spectra (500–750 nm) were monitored with 20 nm slit, 320 nm excitation with 25 nm slit, 50 µs delay, and 400 µs integration times. Excitation spectra (500–700 nm) for Cy5-SA was recorded with 20 nm slit, 750 nm emission with 20 nm slit and 40 µs integration time. Emission spectra (620–800 nm) for Cy5-SA was monitored with 20 nm slit, 580 nm excitation with 20 nm slit and integration time of 40 µs. The absorption spectra for MG and MT2 were monitored from 350 to 800

nm. All measurements were performed in the assay buffer: 50 mM HEPES (pH 7), 150 mM NaCl, 0.05% Triton X-100, and 0.05% BSA. All emission and excitation measurements were performed in Corning low volume 384-well plates in 20 µL final volume using 10 nM concentration of Eu^{3+}-chelate biotin conjugates and Cy5-SA. Absorption spectra for 50 µM MG and MT2 were monitored in clear 96-well plate in 50 µL volume.

2.6 Comparison of 7-, 9-, and 11-dentate Eu^{3+}-chelates in TR-FRET, QRET, and QTR-FRET assays

Analytical performance of the bio7, bio9, and bio11 were compared in a SA binding assay utilizing QRET, TR-FRET, and QTR-FRET methods side-by-side. All biotin assays were performed in 50 µL volume using triplicate reactions in the assay buffer: 50 mM HEPES (pH 7), 150 mM NaCl, 0.05% Triton X-100, and 0.05% BSA. Non-labeled SA was used in QRET and Cy5-SA in TR-FRET and QTR-FRET assays. First we selected the optimal SA concentration for TR-FRET and QRET assays, performing Cy5-SA/SA titration (0.25-16 nM) with or without free biotin (1 µM). Titration was performed with 4 nM Eu^{3+}-biotins. Reactions were incubated for 30 min before time-gated measurement at 615 nm or 665 nm. Thereafter, MT2 quencher was added for the QRET assay before the re-measurement after 10 min of incubation. Next we performed competitive biotin titration (0.050-200 nM) with constant Cy5-SA/SA concentration of 1 and 2 nM, respectively. Cy5-SA/SA and competing biotin were first mixed, following the addition of 4 nM Eu^{3+}-biotins. Reactions were incubated for 30 min before addition of MT2 for QRET or 20 µM MG for QTR-FRET. Signals at 615 nm and 665 nm were monitored before and 10 min after quencher addition in both assays.

2.7 QTR-FRET - quencher ability to reduce donor background

The QTR-FRET assay was developed to eliminate the donor background signal in the TR-FRET assay. We selected bio9 for the QTR-FRET testing and performed bio9 titration at relatively high concentration (4-972 nM) with constant 10 nM Cy5-SA concentration. Cy5-SA was first incubated with or without 3 µM biotin for 5 min and thereafter bio9 was added and incubated for 20 min. Signals were measured at 665 nm before MG was added at concentration of 0-120 µM and signals were re-monitored after 10 min.

2.8 QTR-FRET – Avi-KRAS nucleotide exchange detection

Avi-KRAS assays were performed in 10 µL volume using Corning 384 low volume plates and assay buffer containing 25 mM HEPES (pH 7.5), 1 mM $MgCl_2$, 10 mM NaCl, 0.01% Triton X-100, and 0.005% γ-globulins. Assay was performed with constant Alexa680-SA (20 nM) and SOS^{cat} (10

nM) concentration. Titrated Avi-KRAS (0-1200 nM) was first added to the plate together with Alexa680-SA and either GTP-Eu7 or GTP-Eu9 both used in three concentrations (5 nM, 20 nM or 80 nM). Reaction was initiated by SOS^{cat} and TR-FRET signals at 740 nm were monitored after 20 min. Thereafter, MG was added in a selected Eu^{3+}-chelate dependent concentration (10 µM, 15 µM or 20 µM) and QTR-FRET (740 nm) and QRET (615 nm) signals were monitored after 15 min.

2.9 Data analysis

In all assays, the signal-to-background ratio (S/B) was calculated as μ_{max}/μ_{min}, coefficient of variation (CV%) as $(\sigma/\mu)*100$, and the LOD was defined as $\mu_{min} + 3\sigma$. In all formulas μ is the mean value, and σ is the standard deviation (SD). Data were analyzed using Origin 8 software (OriginLab, Northampton, MA) and the IC_{50} values were obtained using standard sigmoidal fitting functions.

3. Results and discussion

3.1 Assay designs of the different homogeneous energy transfer approaches

We have previously described modified Eu^{3+}-chelate structures to increase the stability and signaling properties of the widely used 7-dentate chelate. Chelates were synthesized by introducing one or two additional iminodiacetate coordinating arms to the original 7-dentate structure [21]. Now, we have performed side-by-side comparison between these chelates to discover differences for their stability and applicability to energy transfer assays. In addition to traditional TR-FRET assay, Eu^{3+}-chelates were compared with a single-label QRET technique and using developed QTR-FRET technique presented here for the first time. The QTR-FRET technique combines the TR-FRET type energy transfer detection from Eu^{3+}-chelates (donor) to Cy5 (acceptor) with the QRET detection principle. QRET concept includes a high concentration soluble acceptor quencher as an energy transfer partner. This molecule can be used to reduce unwanted signal from the non-bound Eu^{3+}-chelate labeled ligand, which therefore can benefit in TR-FRET. The detection principles of these three different detection methods are presented in Figure 1.
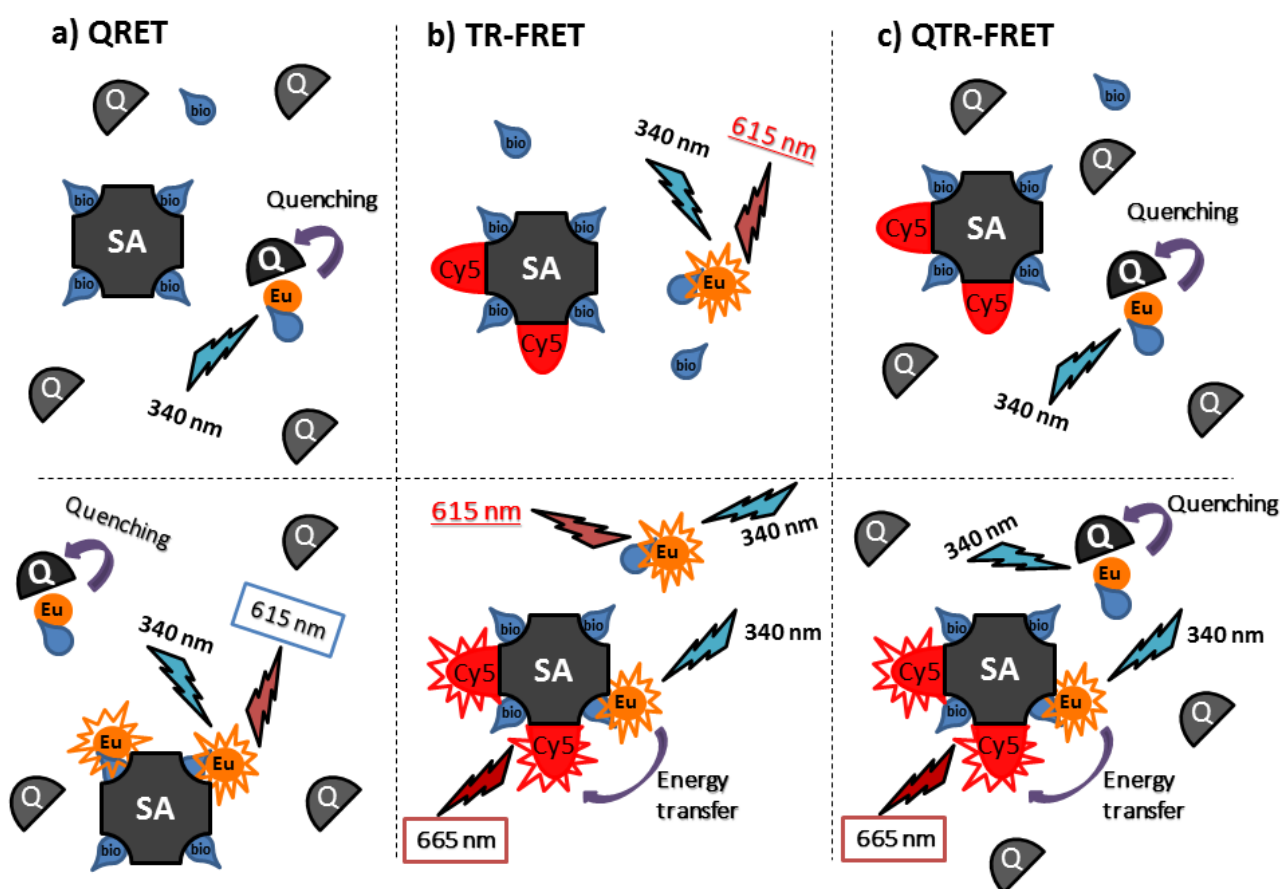
Figure 1. Principles of the homogenous energy transfer based assay systems. (A) QRET: In the absence of excess amount of biotin, the Eu^{3+}-biotin is protected from the soluble quencher upon binding to streptavidin (SA). At high biotin concentration, the protection of the Eu^{3+}-chelate is lost and the Eu^{3+}-signal at 615 nm is lost. (B) TR-FRET: Low biotin concentration leads to high TR-FRET signal at 665 nm due to the close proximity of the SA-Cy5 bound Eu^{3+}-biotin. In the presence of biotin, the TR-FRET signal is decreased due to the increased distance of the donor-acceptor pair. In all cases, excited Eu^{3+}-biotin can cause increased background at 665 nm TR-FRET measurement window. (C) QTR-FRET: In the combined QTR-FRET assay performed in the presence of biotin, introduced soluble quencher reduces the background signal of the non-bound Eu^{3+}-biotin, acting as a second acceptor. With low biotin, high QTR-FRET signal is monitored at 665 nm, and additionally the excess Eu^{3+}-biotin is quenched by the used soluble quencher. This reduces the background signal and improves the detected signal-to-background ratio.

For the comparison of the Eu^{3+}-chelates and the different signaling techniques, we selected SA-biotin interaction as a main model system. This interaction has one of the highest affinities known in nature and it has been widely used to study protein-ligand interactions [25-27]. Due to the ultra-high affinity, the SA-biotin interaction provides rapid low-concentration assays, which we now utilized to demonstrate only the differences between signal readout techniques and signaling properties of the used Eu^{3+}-chelates.

We have previously developed a single-label QRET technology for the monitoring of various protein-ligand interactions [15,22]. In the QRET technique, intact receptor (SA) requires no modification and only Eu^{3+}-conjugation to biotin is required (Figure 1a). The QRET exploit the change in Eu^{3+}-biotin environment when bound to SA or free in solution. Binding changes the local quencher concentration near Eu^{3+}-chelate, enabling the separation between free and bound population. The phenomenon is highly dependent on used quencher molecule and the monitored reaction as shown previously [15,22]. In the traditional TR-FRET method, both SA (Cy5) and biotin (Eu^{3+}-chelate) are labeled and the energy transfer between labels occur only upon Eu^{3+}-biotin binding to Cy5-SA (Figure 1b). In both detection techniques, high signal at either 615 nm (QRET) or 665 nm (TR-FRET) is observed after Eu^{3+}-biotin binding, and signal decrease is observed with an excess of free non-labeled biotin. In case of TR-FRET, weak signal decrease at the donor 615 nm channel can also be detected upon binding, due to energy transfer from donor to acceptor. The novel QTR-FRET technique combines these two detection methods by enabling efficient signal readout at both 615 nm and 665 nm. In QTR-FRET, Cy5-SA, Eu^{3+}-biotin, and soluble quencher are all applied in a single assay (Figure 1c). When compared to TR-FRET, signal from the free non-bound Eu^{3+}-biotin is quenched similarly as in QRET. Thus the Eu^{3+}-chelate background signal in the Cy5-channel at 665 nm is reduced. This background signal is especially relevant at high Eu^{3+}-biotin concentrations as the background signal increases in concentration dependent manner. Due to two distinct energy transfer process in the QTR-FRET technique (Figure 1c), spectral properties of the labels are highly important. Thus in this proof-of-principle work, malachite green (MG) was introduced as a soluble quencher. MG is a suitable selection as it is known to function in the QRET assays, it has highly overlapping absorption spectrum with the Eu^{3+}-chelate main peaks, and MG has basically no fluorescence emission, which could potentially causes interferences (Figure 2) [28]. Depending which detection method is used, the signal monitoring parameters were selected accordingly (See materials and method). In QRET detection, 400 µs delay and integration times were used, as this is the factory setting for Eu^{3+}-signal monitoring in most plate readers. By using shorter delay, we were able to increase the Eu^{3+}-signal to better enable spectral characterization. In TR-FRET and QTR-FRET we selected slightly longer delay (75 µs) as normally used as a factory setting. Selected parameters enabled us to reduce signal levels and enabling all measurements using the same measurement settings.

3.1 Comparison of 7-, 9-, and 11-dentate Eu^{3+}-chelates in TR-FRET, QRET, and QTR-FRET assays
To study the energy transfer properties and functionalities between different chelates, biotin was conjugated to all three chelates, 7-dentate (bio7), 9-dentate (bio9), and 11-dentate (bio11) [21].

Structures and excitation/emission spectra for the Eu^{3+}-chelates are presented in (Figure 2). All three Eu^{3+}-chelates share the same basic structure and showed the characteristic excitation peak at 320-325 nm. Eu^{3+}-chelates share also the same two emission peaks, main peak at 615-620 nm and the secondary peak at 695-700 nm. Cy5-SA showed excitation maximum at 655 nm and the spectra clearly overlaps with the Eu^{3+}-chelate main emission peak (Figure 2). This enabled TR-FRET assay using Eu^{3+}-chelate as a donor and Cy5 as an acceptor fluorophore. TR-FRET is monitored at 665 nm, near the Cy5-SA emission maximum at 672 nm. In the QRET assay, MT2 absorption maximum was monitored at 520 nm and the spectra overlaps with Eu^{3+}-chelate emission (data not shown). However, it has emission maximum at 665 nm and thus it cannot be applied in QTR-FRET assay measured at 665 nm (data not shown). Unlike MT2, MG has basically no emission but completely overlapping absorption spectra with Eu^{3+}-chelate main emission peak. This maximum at 616 nm makes it ideal for QTR-FRET assays (Figure 2).
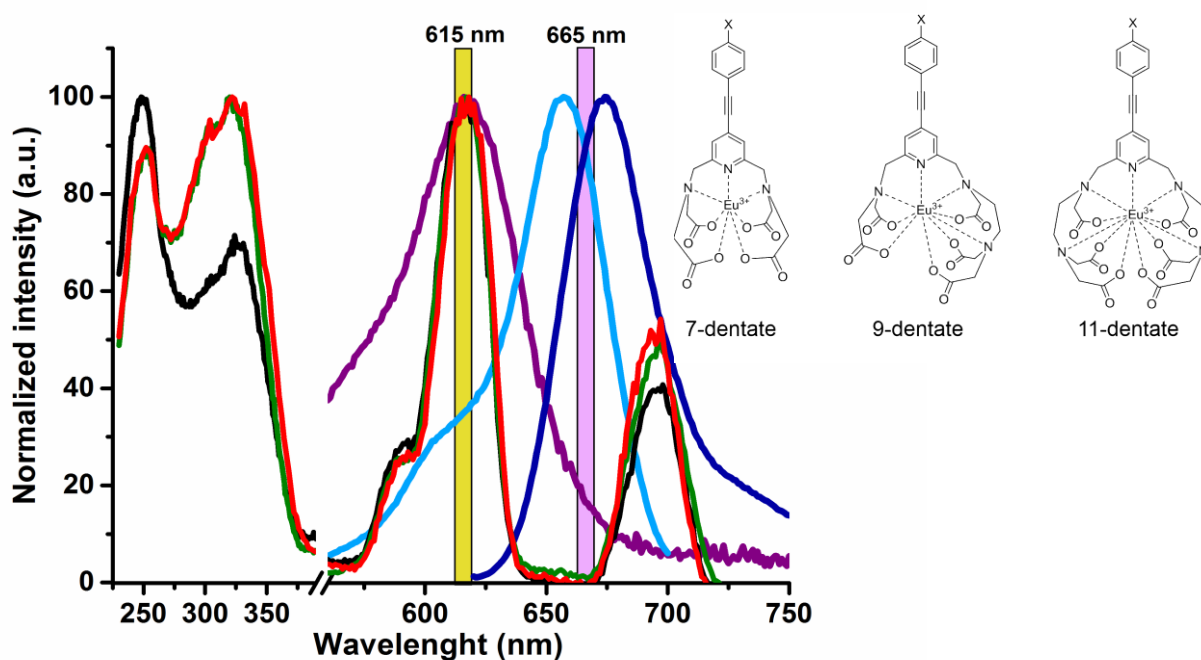

Figure 2. Normalized spectra for the assay components and the 7-, 9-, and 11-dentate Eu^{3+}-chelate structures. Time-gated excitation and emission spectra for bio7 (black), bio9 (green), and bio11 (red) showed characteristic excitation peak at 320 nm and two emission peaks at 615 nm and 695 nm. Cy5-SA excitation (light blue) clearly overlap with the Eu^{3+}-chelate main emission peak, enabling energy transfer and TR-FRET monitoring at Cy5-SA emission wavelength (dark blue). Absorption spectra for MG (purple) completely overlap with the Eu^{3+}-chelate main emission peak, enabling efficient quenching of the Eu^{3+}-signal in QTR-FRET. In QRET assay the signal were monitored at 615 nm and in TR-FRET and QTR-FRET at 665 nm. In the Eu^{3+}-chelate structures X refers to $NHCSNH(CH_2)_3NH$-biotin.

First, the QRET and TR-FRET assays were optimized for bio7, bio9, and bio11 and for SA or SA-Cy5 concentrations, respectively. In the QRET method with all Eu^{3+}-biotin constructs, the highest S/B ratios were monitored with 2 nM SA (Figure 3a). At higher SA concentrations, a slight decrease in the S/B ratio was monitored especially with bio7 and bio9. The QRET assays preferred the 9-dentate chelate, showing the highest S/B of 17 ± 1 followed by 11 ± 1 and 8 ± 1 for bio11 and bio7, respectively. In the TR-FRET assay, 1 nM Cy5-SA was already sufficient to produce the maximal S/B ratio (Figure 3b). Unlike in the QRET, bio7 provided the highest S/B ratio of 20 ± 1 in the TR-FRET assay. The two more stable chelate constructs showed nearly equal performance in the TR-FRET with S/B ratios of 16 ± 1 and 15 ± 1 for bio11 and bio9, respectively [21,29]. As in the QRET assay, the observed S/B ratio decreased at higher Cy5-SA concentrations (Figure 3). The optimal SA concentration difference between QRET and TR-FRET, 2 nM or 1 nM, is not significant and can be due to the difference in the concentration measurement after labeling. Unrelatedly to the monitored energy transfer signal, bio7 was partly quenched (~40 % signal lost) upon binding to the non-modified SA without the quencher. This SA binding induced quenching effect is also seen with bio9 (~10 % signal lost), but not with bio11 (data not shown). In other words, the observed S/B ratio before quencher addition is below 1 in the QRET assay. This binding induced quenching with bio7 might be due to relative short luminescence lifetime of 0.39 ms with this chelate, compared to 1.15 ms and 1.07 ms with bio9 and bio11, respectively [21]. Observed quenching can also partly explain the better functionality of the bio9 and bio11 compared to bio7, but this SA-interaction induced quenching effect is expected to be strictly case specific and relate only to this SA-biotin system. In the current assay setups, SA-interaction induced quenching has a negative effect on Eu^{3+}-chelate functionality, but this does not entirely explain the better functionality of bio9 compared to bio7 in the QRET assay. In the TR-FRET assay the functionality of bio7 prevails bio9 despite the binding induced quenching. In fact the reduced bio7 background signal may contribute to the improved functionality of bio7 especially in the TR-FRET approach.
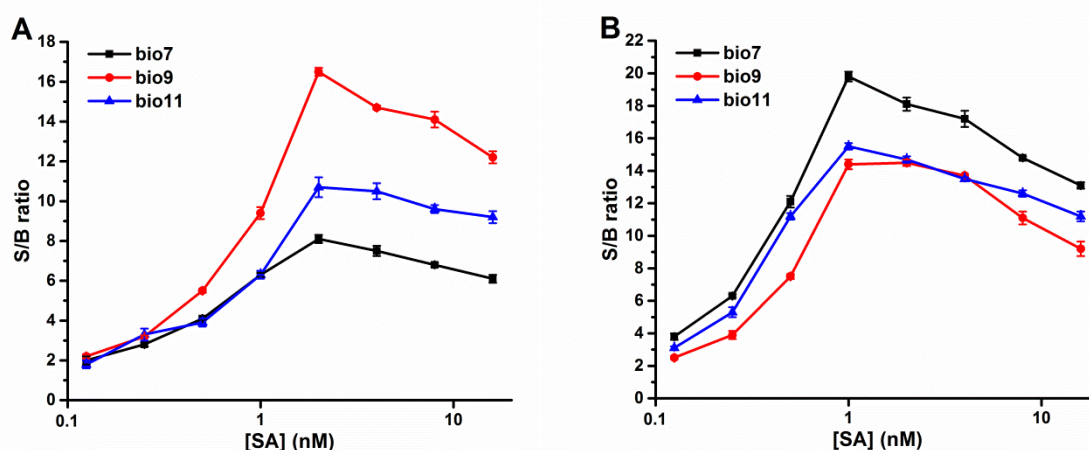
Figure 3. Functionality of the Eu^{3+}-biotin conjugates, bio7, bio9, and bio11, in SA titration. Biotin conjugated with 7- (black), 9- (red), and 11-dentate (blue) Eu^{3+}-chelates (4 nM) were tested with no competing biotin or with 1 µM biotin using varying SA (QRET) or Cy5-SA (TR-FRET) concentrations. The S/B ratios were monitored using QRET readout at 615 nm (A) and TR-FRET readout at 665 nm (B). Data represent mean ± SD (n=3).

Next we performed biotin titration with all three Eu^{3+}-biotin constructs to define analytical performance for biotin detection using TR-FRET, QRET, and QTR-FRET. Biotin titrations were performed with 1 nM Cy5-SA which was shown to be optimal to TR-FRET and thus expected to be optimal also to QTR-FRET readout. Also in QRET, non-optimal 1 nM SA was used to enable direct comparison (Figure 3a). To our surprise, bio7, which showed the highest S/B ratio in the TR-FRET readout (Figure 4a), resulted no change in the S/B ratio in the QTR-FRET assay after quencher addition (14 ± 1 vs. 14 ± 1) (Figure 4b). In the QTR-FRET assay, bio9 showed the highest S/B ratio and also the largest improvement in the S/B ratio (12 ± 1 vs. 18 ± 1) after MG addition. This improvement was expected as bio9 performed well already in the QRET assay (Figure 4c). Based on these results, the QTR-FRET performance ranking order of the Eu^{3+}- biotins followed that as in the QRET assay. This was found with both quenchers, MT2 or MG, and whether the signal readout was carried out at 615 or 665 nm in the QRET and QTR-FRET assays, respectively (Figure 4). S/B ratios in QRET were lower than with the two other methods, which was expected due to non-optimal 1 nM SA concentration (Figure 3a). Using the optimal 2 nM SA, the S/B ratios monitored in QRET were doubled (data not shown). In all assays, bio11 showed average functionality and also its direct Eu^{3+}-signal level is in between of bio9 and bio7, showing the highest and the lowest Eu^{3+}-signal, respectively (data not shown). As the same SA concentration (1 nM) was used in all assays, no major difference between methods and chelates were expected. In TR-FRET, the IC_{50} values with bio7, bio9, and bio11 were between 1.7 and 2.5 nM, and similarly in QRET and QTR-FRET the IC_{50} values were from 1.3 to 1.6 nM and from 0.6 to 2.3 nM, respectively.
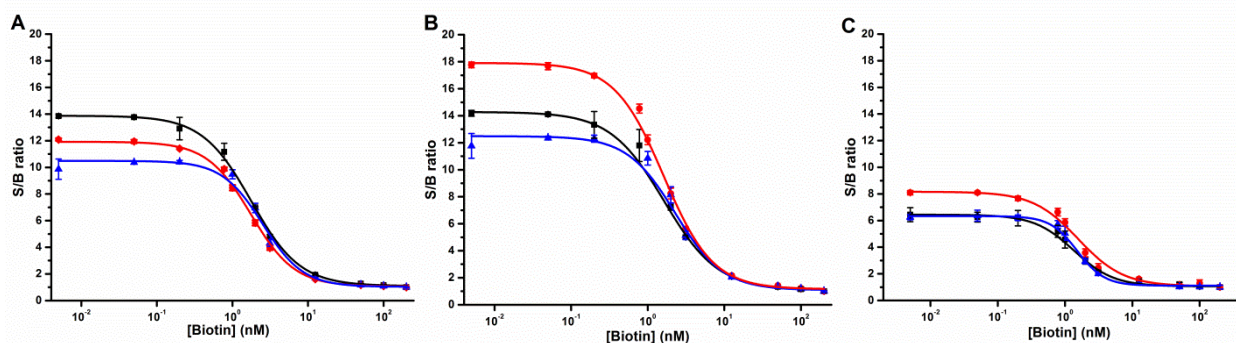
Figure 4. Biotin calibration curves for Eu^{3+}-biotin conjugates utilizing different detection method. Biotin-complexes (4 nM), bio7 (black), bio9 (red), and bio11 (blue), were used in biotin titration with three different readout methods. Titrations were performed using 1 nM Cy5-SA and detected using TR-FRET (A) or QTR-FRET (B) readout at 665 nm. QRET assay was performed using non-optimal 1 nM SA and the results were monitored at 615 nm (C). Data represent mean $\pm$ SD (n=3).

3.3 QTR-FRET - quencher functionality in donor background signal reduction

As the bio9 showed improved performance compared to bio7 and bio11 in both QRET and QTR-FRET assays, it was selected for further characterization of the QTR-FRET assay. All previous assays were performed with relatively low 4 nM Eu^{3+}-chelate concentration allowing near complete binding to SA due to the high biotin-SA interaction affinity [25-27]. Thus, the QTR-FRET was not expected to improve significantly the TR-FRET functionality under these conditions. However, complete binding of all ligands is not often the case with biologically more relevant ligands, and thus we decided to demonstrate the QTR-FRET detection at high concentration excess of bio9 compared to Cy5-SA binding capacity. As the QTR-FRET approach is based on quenching of the non-bound Eu^{3+}-chelate conjugated ligand, the method is expected to be beneficial under these "non-optimal" conditions leading to improved detectability of low affinity ligands and also improving functionality in solutions containing impurities or other interfering factors.

To prove our hypothesis, bio9 concentration was titrated in the presence of increasing quencher concentration. We found a clear increase in S/B ratio due the decrease in free Eu^{3+}-biotin derived background signal (Figure 5a). In TR-FRET assay, 4-36 nM bio9 gave nearly equal S/B ratio from 12 ± 1 to 13 ± 1. However, the ratio was dramatically decreased when bio9 concentration was further increased, as free bio9 induced background signal monitored at 665 nm measurement window was increased. This problem would be even more dramatic if the spectral overlap between donor and acceptor is greater. In the QTR-FRET, quencher reduces the background arising from the non-bound bio9 and increase in S/B ratio was monitored with all bio9 concentrations (Figure 5b). The optimal S/B ratio was observed using approx. 60 µM concentration of MG, except with the lowest bio9 concentration. At 4 nM bio9 concentration used in all previous assays, the 60 µM MG

13

concentration was already too high reducing dramatically also the specific signal when assayed with 10 nM Cy5-SA. When signal behavior was evaluated, the quencher effect to the bound bio9 fraction was found to be linear, as the effect on free bio9 was more drastic. The observed S/B maximum was reached when the free bio9 signal was quenched near the buffer background level (Figure 5c). As the optimum was reached at nearly equal quencher concentration with various bio9 concentrations, SA bound bio9 can be expected to be well protected and only free bio9 is efficiently quenched. Also the optimization of the assay is simplified, thus changes in bio9 concentration do not significantly effect on the optimal quencher concentration but the binding capacity of the receptor, here SA, determines the used quencher concentration. However, this is expected to be true only in special cases, in which the dissociation rate of the ligand is slow. In the QTR-FRET, the S/B ratio increased 4-fold or more when bio9 concentration over 12 nM was used. The highest increase in S/B ration after introduction of MG, over 7-fold, was observed with 330 nM bio9 (Figure 5b).
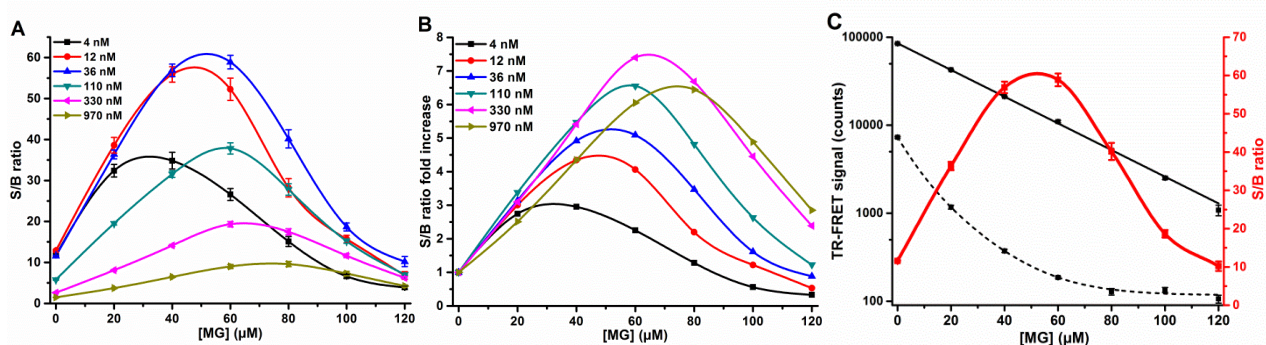

Figure 5. Effect of the soluble quencher and bio9 concentration using the QTR-FRET assay. (A) Increasing bio9 concentration provides high specific and background signal at 665 nm when assayed with 10 nM Cy5-SA and without the soluble quencher (MG). The improved S/B ratio (with or without 3 µM biotin) was found until the bio9 concentration exceeded 36 nM. (B) Soluble quencher (MG) partially overcomes the background signal increase by quenching the non-bound bio9. Quenching related positive effect can be observed with all bio9 concentrations. (C) Increase of MG concentration induces linear TR-FRET quenching (solid black) when assayed with Cy5-SA (10 nM) and bio9 (36 nM). The response was more drastic in the presence of competing biotin (dashed black) as bio9 was free in solution and exposed to quencher. Thus the increase in the S/B ratio (red) is observed until the buffer background signal is reached. Data represent mean ± SD (n=3).

Biotin-SA interaction is widely used research tool due to the high interaction affinity, but to show assay function in more biologically relevant context we selected KRAS as a second target [30]. In all previous assays we used Cy5 as an energy transfer acceptor, but to further broaden the QTR-FRET applicability we selected Alexa680-SA for KRAS assay monitoring at 740 nm. For KRAS assays, 7- and 9-dentate Eu^{3+}-chelate were conjugated to GTP (GTP-Eu7 and GTP-Eu9) [24]. In the assay, GTP-Eu7 and GTP-Eu9 were loaded to Avi-KRAS in the presence of SOS[cat] enabling the

nucleotide exchange reaction [24,31]. The TR-FRET signal was monitored for Avi-KRAS bound Alexa680-SA after GTP-Eu loading. With GTP-Eu7, minor negative effect to detected S/B ratio was monitored, when its concentration was increased from 5 nM to 80 nM (Figure 6a). As expected, addition of MG rescued the S/B ratio by reducing the background signal. At the highest GTP-Eu7 concentration the improvement between TR-FRET and QTR-FRET was already nearly 3-fold. Similar results were recorded with GTP-Eu9, which showed over 3-fold improvement in S/B ratio at the highest GTP-Eu concentration (Figure 6b). There were no major S/B ratio difference between GTP-Eu7 and GTP-Eu9 in TR-FRET, but more drastic improvement in the presence of MG was monitored with GTP-Eu9. These QTR-FRET results were in line with the results obtained with biotin-SA system. Sensitivity of the Avi-KRAS assay was significantly improved only in case of 80 nM GTP-Eu (data not shown). However, this was also expected as the GTP affinity to KRAS is at pM level, and in case of the GTP-Eu9 at low nM level [24,32]. Even over main interest in QTR-FRET was to reduce the Eu^{3+}-signal derived background in TR-FRET, it also enables the signal readout directly from the Eu^{3+}-signal at 615 nm as in the QRET detection. This was demonstrated with GTP-Eu9 monitored also at 615 nm (Figure 6c). This ability for dual-wavelength detection from the same assay well potentially enables coupled assays for multianalyte applications to measure different binding events. This could be true when acceptor label is conjugated to third molecule other than Eu^{3+}-ligand interaction partner.
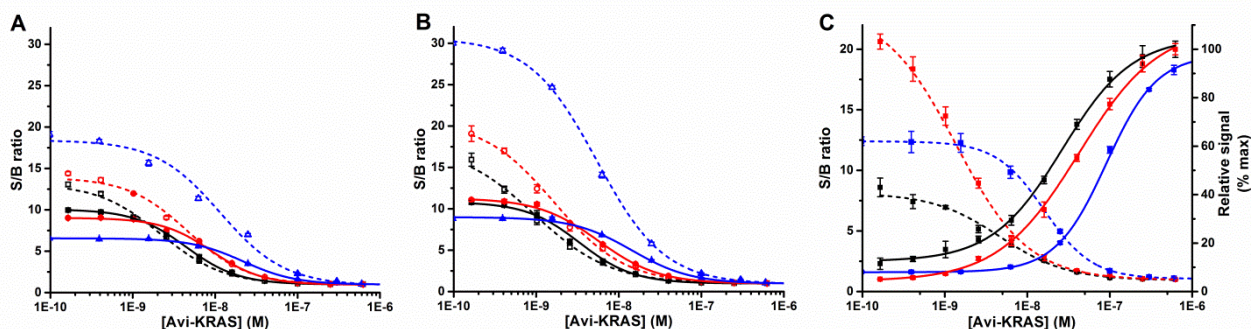

Figure 6. Avi-KRAS titration detected with TR-FRET, QTR-FRET, and QRET. Avi-KRAS titration was performed with 5 nM (black), 20 nM (red), and 80 nM (blue) GTP-Eu7 (A) or GTP-Eu9 (B) concentrations, in the presence of constant 10 nM SOS[cat] and 20 nM Alexa680-SA. Low Avi-KRAS concentration produced high S/B ratio when compared to high Avi-KRAS when TR-FRET (solid line) was monitored at 740 nm after 15 min of incubation. Thereafter, MG (10-20 µM) quencher was added and the improved QTR-FRET (dashed line) results were monitored at 740 nm. After MG addition, also the QRET at 615 nm was monitored and the Avi-KRAS concentration dependent GTP-Eu9 binding was recorded (C). Data represent mean ± SD (n=3).

Directly luminescent Ln^{3+}-chelates are widely used in different bioanalytical applications as an energy transfer donors or directly as a only used label [4-9,12-16]. We have now compared three different Eu^{3+}-chelates to link the increase in stability and luminescence signal to the overall functionality of the assay. As found in TR-FRET assays, the increased stability seems to weaken the energy transfer properties of the chelate, even the Eu^{3+}-signal was increased. However, the same observation does not hold for energy transfer processes occurring in a different manner, as in the QRET and QTR-FRET approaches, where soluble quencher is introduced at high concentration. In these applications, one additional protective iminodiacetate coordinating arm of (bio9 or GTP-Eu9) was found beneficial. The second coordinating arm decreased the overall brightness of the chelate, and its function as an energy transfer donor. This indicates the importance of the Eu^{3+}-chelate selection in different bioanalytical applications using different signal readouts. The QTR-FRET approach, showed similar Eu^{3+}-chelate preference as the QRET technology [15,22,23]. This seems not to be due to single quencher, as different quenchers were used in the QRET and QTR-FRET. We expect that the increase in assay functionality showed with the QTR-FRET approach, can be directly applied to other TR-FRET assays and found extremely useful in this type of applications. This was already shortly demonstrated with Avi-KRAS and a second acceptor molecule (Alexa680). As with Eu^{3+}-biotin, Avi-KRAS assay showed improved analytical performance after the MG quencher was introduced. Both QTR-FRET and QRET signals were also measurable after MG addition, which indicates the potential to monitor two binding events in addition to the ability to reduce TR-FRET background signal.

4. Conclusions

We have performed side-by-side comparison of three Eu^{3+}-chelates in different energy transfer applications. Eu^{3+}-chelates showed different stability and also their signaling properties improved together with their increased stability. However, this was found not to be beneficial to energy transfer applications, leading eventually to reduced functionality. We introduced a novel QTR-FRET method to reduce background luminescence occurring from the excess of Eu^{3+}-conjugated ligand. Addition of soluble quencher efficiently reduced the background from non-bound Eu^{3+}-ligand, and thus QTR-FRET is expected to be especially useful in assays where high Eu^{3+}-ligand concentration is needed. As shown with Avi-KRAS, QTR-FRET also serves a potential method for multiplexing. In the dual-binding assay the first binding event, e.g. between protein and small Eu^{3+}-ligand, is monitored at 615 nm (QRET) and the second binding at acceptor emission window (QTR-FRET). This work clearly shows the functionality of the Eu^{3+}-chelates in different bioanalytical applications and highlights the importance of the Eu^{3+}-chelate selection for the specific application.

Acknowledgement

Competing financial interests

The authors declare the following competing financial interest(s): Kari Kopra and Harri Härmä have commercial interest through QRET Technologies Ltd.

AUTHOR INFORMATION

Corresponding Author

*kari.kopra@utu.fi

ORCID

Kari Kopra: 0000-0001-7585-6020

REFERENCES

[1] I. L. Mendintz, N. Hildebrandt, FRET - Förster resonance energy transfer: from theory to applications Wiley-VCH, (2013) 1-816.

[2] L. Ma, F. Yang, J. Zheng, Application of fluorescence resonance energy transfer in protein studies, J. Mol. Struct. 1077 (2014) 87-100.

[3] D. Shrestha, A. Jenei, P. Nagy, G. Vereb, J. Szöllősi, Understanding FRET as a research tool for cellular studies, Int. J. Mol. Sci. 16 (2015) 6718-6756.

[4] L.E. Morrison, Time-resolved detection of energy transfer theory and application to immunoassays, Anal. Biochem. 174 (1988) 101-120.

[5] F. Degorce, A. Card, S. Soh, E. Trinquet, G. P. Knapik, B. Xie, HTRF: A technology tailored for drug discovery – A review of theoretical aspects and recent applications, Curr. Chem. Genomics. 3 (2009) 22-32.

[6] E. Ergin, A. Dogan, M. Parmaksiz, A. E. Elçin, Y. M. Elçin, Time-resolved fluorescence resonance energy transfer [TR-FRET] assays for biochemical processes, Curr. Pharm. Biotechnol. 17 (2016) 1222-1230.

[7] M. Sy, A. Nonat, N. Hildebrandt, L. J. Charbonnière, Lanthanide-based luminescence biolabelling. Chem. Commun. 52 (2016) 5080-5095.

[8] J. M. Zwier, N. Hildebrandt, Time-gated FRET detection for multiplexed biosensing. In: Geddes C. (eds) Reviews in Fluorescence 2016. Reviews in Fluorescence. Springer, (2017) 17-43.

[9] U. Cho, D. P. Riordan, P. Ciepla, K. S. Kocherlakota, J. K. Chen, P. B. Harbury, Ultrasensitive optical imaging with lanthanide lumiphores. Nat. Chem. Biol. 14 (2018) 15-21.

[10] H. Siitari, I. Hemmilä, E. Soini, T. Lövgren, V. Koistinen, Detection of hepatitis B surface antigen using time-resolved fluoroimmunoassay, Nature. 301 (1983) 258-260.

[11] I. Hemmilä, S. Dakubu, V-M. Mukkala, H. Siitari, T. Lövgren, Europium as a label in time-resolved immunofluorometric assays, Anal. Biochem. 137 (1984) 335-343.

[12] M. Latvala, H. Takalo, K. Simberg, J. Kankare, Enhanced Eu^{III} ion luminescence and efficient energy transfer between lanthanide chelates within the polymeric structure in aqueous solutions, J. Chem. Soc. Perkin Trans. 2 5 (1995) 995-999.

[13] H. Härmä, L. Dähne, S. Pihlasalo, J. Suojanen, J. Peltonen, P. Hänninen, Sensitive quantitative protein concentration method using luminescent resonance energy transfer on a layer-by-layer europium(III) chelate particle sensor, Anal. Chem. 80 (2008) 9781-9786.

[14] D. Geißler, S. Linden, K. Liermann, K. D. Wegner, L. J. Charbonnière, N. Hildebrandt, Lanthanides and quantum dots as Förster resonance energy transfer agents for diagnostics and cellular imaging. Inorg. Chem. 25 (2014) 1824-1838.

[15] K. Kopra, H. Härmä, Quenching resonance energy transfer (QRET): a single-label technique for inhibitor screening and interaction studies, N. Biotechnol. 32 (2015) 575-580.

[16] C. Chen, L. Ao, Y. T. Wu, V. Cifliku, M. Cardoso Dos Santos, E. Bourrier, M. Delbianco, D. Parker, J. M. Zwier, L. Huang, N. Hildebrandt, Single-nanoparticle cell barcoding by tunable FRET from lanthanides to quantum dots. Angew. Chem. Int. Ed. Engl. 57 (2018) 13686-13690.

[17] T. Heyduk, Measuring protein conformational changes by FRET/LRET, Curr. Opin. Biotechnol. 13 (2002) 292-296.

[18] V. Laitala, I. Hemmilä, Homogeneous assay based on anti-stokes' shift time-resolved fluorescence resonance energy-transfer measurement, Anal. Chem. 77 (2005) 1483-1487.

[19] J. Vuojola, U. Lamminmäki T. Soukka, Resonance energy transfer from lanthanide chelates to overlapping and nonoverlapping fluorescent protein acceptors, Anal. Chem. 81 (2009) 5033-5038.

[20] K. Kopra, V. Eskonen, T. Seppälä, J. Jakovleva, R. Huttunen, H. Härmä, Peptic fluorescent "signal-on" and "signal-off" sensors utilized for the detection protein post-translational modifications. ACS Omega. 4 (2019) 4269-4275.

[21] Q. Wang, K. N. Nono, M. Syrjänpää, L. J. Charbonnière, J. Hovinen, H. Härmä, Stable and highly fluorescent Europium(III) chelates for time resolved immunoassays, Inorg. Chem. 52 (2013) 8461-8466.

[22] H. Härmä, A. Rozwandowicz-Jansen, E. Martikkala, H. Frang, I. Hemmilä, N. Sahlberg, V. Fey, M. Perälä, P. Hänninen, A new simple cell-based homogeneous time-resolved fluorescence QRET technique for receptor-ligand interaction screening, J. Biomol. Screen. 14 (2009) 936-943.

[23] K. Kopra, M. Syrjänpää, P. Hänninen, H. Härmä, Non-competitive aptamer-based quenching resonance energy transfer assay for homogeneous growth factor quantification, Analyst. 139 (2014) 2016-2023.

[24] K. Kopra, A. Ligabue, Q. Wang, M. Syrjänpää, O. Blaževitš, S. Veltel, A. J. van Adrichem, P. Hänninen, D. Abankwa, H. Härmä, A homogeneous quenching resonance energy transfer assay for the kinetic analysis of the GTPase nucleotide exchange reaction. Anal. Bioanal. Chem. 406 (2014) 4147-4156.

[25] M. Wilchek, E. A. Bayer, The avidin-biotin complex in bioanalytical applications, Anal. Biochem. 171 (1988) 1-32.

[26] M. González, L. A. Bagatolli, I. Echabe, J. L. Arrondo, C. E. Argaraña, C. R. Cantor, G. D. Fidelio, Interaction of biotin with streptavidin. Thermostability and conformational changes upon binding, J. Biol. Chem. 272 (1997) 11288-11294.

[27] P. S. Stayton, S. Freitag, L. A. Klumb, A. Chilkoti, V. Chu, J. E. Penzotti, R. To, D. Hyre, I. Le Trong, T. P. Lybrand, R. E. Stenkamp, Streptavidin-biotin binding energetics, Biomol. Eng. 16 (1999) 39-44.

[28] K. Kopra, Shweta, E. Martikkala, P. Hänninen, U. Petäjä-Repo, H. Härmä, A homogeneous single-label quenching resonance energy transfer assay for a δ-opioid receptor-ligand using intact cells, Analyst. 138 (2013) 4907-4914.

[29] P. Hänninen, H. Härmä, Lanthanide luminescence: Photophysical, analytical and biological aspects, Springer Ser. Fluoresc. Springer-Verlag, Berlin, 2011.

[30] L. Goitre, E. Trapani, L. Trabalzini, S. F. Retta, The Ras superfamily of small GTPases: the unlocked secrets. Methods Mol. Biol. 1120 (2014) 1-18.

[31] K. Kopra, A. J. van Adrichem, O. M. H. Salo-Ahen, J. Peltonen, K. Wennerberg, H. Härmä, High-throughput dual screening method for Ras activities and inhibitors. Anal. Chem. 89 (2017) 4508-4516.

[32] J. C. Hunter, A. Manandhar, M. A. Carrasco, D. Gurbani, S. Gondi, K. D. Westover, Biochemical and structural analysis of common cancer-associated KRAS mutations. Mol. Cancer Res. 13 (2015) 1325-1335.

TOC: